

# GADMSL: Graph Anomaly Detection on Attributed Networks via Multi-scale Substructure Learning

Jingcan Duan, Siwei Wang, Xinwang Liu, Haifang Zhou, Jingtao Hu, Hu Jin

*Abstract*—Recently, graph anomaly detection has attracted increasing attention in data mining and machine learning communities. Apart from existing attribute anomalies, graph anomaly detection also captures suspicious topological-abnormal nodes that differ from the major counterparts. Although massive graph-based detection approaches have been proposed, most of them focus on node-level comparison while pay insufficient attention on the surrounding topology structures. Nodes with more dissimilar neighborhood substructures have more suspicious to be abnormal. To enhance the local substructure detection ability, we propose a novel Graph Anomaly Detection framework via Multi-scale Substructure Learning (GADMSL for abbreviation). Unlike previous algorithms, we manage to capture anomalous substructures where the inner similarities are relatively low in dense-connected regions. Specifically, we adopt a region proposal module to find high-density substructures in the network as suspicious regions. Their inner-node embedding similarities indicate the anomaly degree of the detected substructures. Generally, a lower degree of embedding similarities means a higher probability that the substructure contains topology anomalies. To distill better embeddings of node attributes, we further introduce a graph contrastive learning scheme, which observes attribute anomalies in the meantime. In this way, GADMSL can detect both topology and attribute anomalies. Ultimately, extensive experiments on benchmark datasets show that GADMSL greatly improves detection performance (up to 7.30% AUC and 17.46% AUPRC gains) compared to state-of-the-art attributed networks anomaly detection algorithms.

*Index Terms*—Graph Anomaly Detection, Network Substructure, Attributed Networks, Graph Neural Networks.

## I. INTRODUCTION

Attributed networks have the powerful capability of modeling and analyzing numerous complex scenarios in the real world. In recent years, researches [1]–[5] on attributed networks tasks are becoming an increasingly appealing direction for academia and industry. In particular, anomaly detection has constantly been a vital topic in attributed networks [6], which has ubiquitous applications in many fields, such as financial fraud detection [7], social spam detection [8], network intrusion detection [9], information system error detection [10], etc.

Attributed networks anomaly detection termed ANAD intends to discern anomalous samples that diverge from frequent patterns. Usually, samples refer to the nodes in the network [11]. Unlike the raw data widely applied in other fields, attributed networks include both node attribute and network topology information. Concretely, the node attribute information is often high-dimensional with diverse representations. The network topology information reflects the connection relationships between the inner nodes. Inspired by the previous literature [12]–[14], the mismatch between the above two types

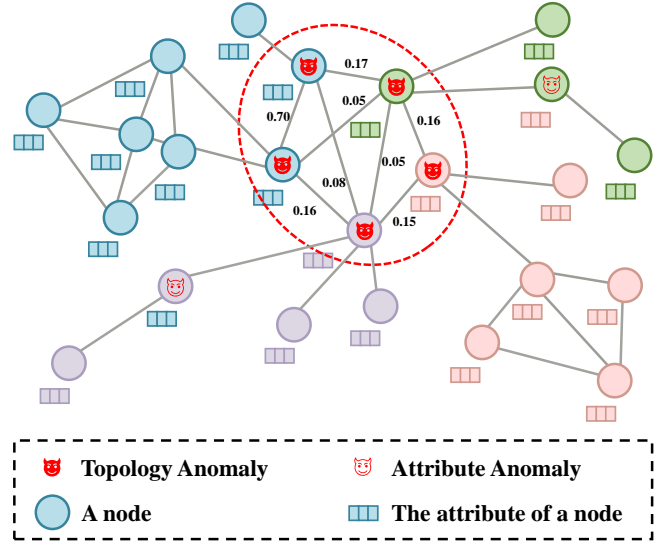


Figure 1: The toy example contains two typical anomalous nodes in attributed networks: (1) Topology anomaly: closely connected nodes with dissimilar attribute values in the red circle. The number on edge indicates the attribute similarity of the two nodes. (2) Attribute anomaly: nodes with dissimilar attribute values from neighborhoods.

of information will cause two typical kinds of anomalies. As illustrated in Figure 1, the topology anomaly has normal attribute values at a glance, while it can be found in a dense substructure with low inner similarities; on the contrary, the attribute counterpart has a normal neighborhood connectivity relationship, while its attribute values may be contaminated by noise and are not similar to the neighborhoods. Further analysis demonstrates that the pattern of topology anomalies is the collective behavior of a group of anomalous nodes, while attribute anomalies show individual behavior.

To avoid the labor-intensive and time-consuming cost of collecting node labels, ANAD algorithms usually adopt the unsupervised learning paradigm in practice. Early shallow methods [15]–[19] mine either node attribute information or network topology information to discover anomalous node patterns that deviate from the majority of nodes by traditional machine learning. Witnessing the success of deep learning in recent years, the deep approaches have made plentiful progress by integrating neural networks into the ANAD field. This promising strategy encourages researchers to design various deep neural network architectures, such as reconstruction tasks [20], reinforcement learning tasks [21], self-supervised

pretext tasks [22]–[25], etc.

Despite the fruitful progress of ANAD, it remains two critical issues: **(1)** *Current methods do not simultaneously attach importance to both the node attribute and network topology information*. The majority of shallow methods, limited by their thoughtless consideration, can only use either attribute or topology information. Besides, most deep anomaly detection methods based on GNN focus more on the node attribute values but sometimes less on the equally important network topology information. Due to the above two reasons, existing methods still suffer from poor performance on all kinds of anomalies. **(2)** *Previous approaches generally adopt suboptimal patterns to detect topology anomalies*. Although some recent works (e.g., SCAN [16]) pay attention to network topology information, they lack sufficient abilities to explore intricate topology anomalies. Anomalous substructures can be defined as areas with relatively low inner-node similarities but dense edges inside. Detecting anomalous substructure can capture the collective anomalous behavior of nodes. Obviously, it is a more effective way to detect the collective anomalous behavior of topology anomalies by anomalous substructures perception that has not been exploited in past works. Besides, most previous models only employ AUC values as the evaluation metric. However, AUC is biased without comprehensive considerations. A higher AUC value reflects that a randomly chosen anomaly receives a higher score than a normal node. Even though AUC reveals the capability of the model to a certain extent, it underperforms in some scenarios. On the one hand, it cannot accurately reflect the model performance with the unbalanced positive and negative data. On the other hand, it fails to detailedly reflect the recall and accuracy rate [26] that can be fatal in some cases such as spam detection, network attack detection, etc. These scenarios call for more comprehensive evaluation metrics to demonstrate the detection ability of the model under different settings.

Recently, CoLA [24] has become a strong baseline in ANAD that adopts a contrastive learning framework to detect both topology and attribute anomalies. Nevertheless, the performance of topology anomaly detection can still be improved. The local information around nodes can be considered one of the most critical information in ANAD [24]. However, the random walk-based (usually 3-hop in CoLA) subgraph sample method cannot capture adequate local topology information because of its randomness and parameter-fixed. In extreme cases, it may obtain counterproductive information. Meanwhile, CoLA implements anomaly detection by contrasting the node and subgraph attributes. It performs well when detecting attribute anomalies but fails to integrate enough topology information when detecting topology anomalies. Hence, how to design a better method of discerning all kinds of anomalies, especially using node-local topology information, is imperative to solve in ANAD tasks. It is a promising solution that first discovers anomalous substructures to excavate more local topology information and then measures inner-node pair attribute similarity to utilize the local attribute information.

To this end, we propose a novel **Graph Anomaly Detection** framework via **Multi-scale Substructure Learning (GADMSL)** for abbreviation), which both detects the topology and attribute

anomaly concurrently. The framework of our proposed method is shown in Figure 2. To remedy the deficiency of existing methods, our insight is to propose an effective topology anomaly detection paradigm. First, we leverage a density-based algorithm in the region proposal module to discover high-density substructures as suspicious regions. Next, the overall anomaly degrees of the substructures are obtained by measuring the similarity degree of inner-node embeddings. Substructures with lower inter-node embedding similarities are more likely to obtain topology anomalies. Then, to distill better embeddings of node attributes for similarity measure, we employ a contrastive learning scheme rather than suboptimal reconstruction or reinforcement learning methods. The obtained embeddings further perform excellently in detecting attribute anomalies. Finally, the aggregator combines the topology and attribute anomaly information to compute the final anomaly score for each node. It is worth noting that we design a new multi-scale scoring strategy during topology anomaly score calculation. In general, GADMSL can discern both the topology and attribute anomaly simultaneously. Extensive evaluations and comprehensive metrics on benchmarks show its astonishing effectiveness compared to strong competitors.

In general, the main contributions of this work are summarized below:

- We redesign the new principle to detect the topology anomalies by perceiving the anomalous substructures of the network. To the best of our knowledge, we are among the first to design a substructure-based mechanism as a new topology anomaly detection paradigm.
- Comparing to existing approaches, a generalized framework termed GADMSL is proposed, which can be concurrently aware of node attribute information and network topology information. Therefore, GADMSL experts in detecting both topology and attribute anomalies simultaneously.
- Experiments demonstrate the remarkable advantage of GADMSL against current attributed networks anomaly detection counterparts, which indicates the importance of both topology and attribute information.

## II. RELATED WORK

In this section, we will review the related work in terms of (1) attributed networks anomaly detection; and (2) graph contrastive learning.

### A. Attributed Networks Anomaly Detection

An attributed network is a structured network with multidimensional attribute information. Many traditional algorithms have been proposed in ANAD. They are based on the non-deep anomaly detection way, which captures anomalous patterns from either topology or node attributes of the network. LOF [15] and Radar [18] find the differences in attributes between the target node and the context or most of the nodes. Among the methods based on topology information, SCAN [16] is one of the most well-known works. AMEN [17] and ANOMALOUS [19] both use node attribute information

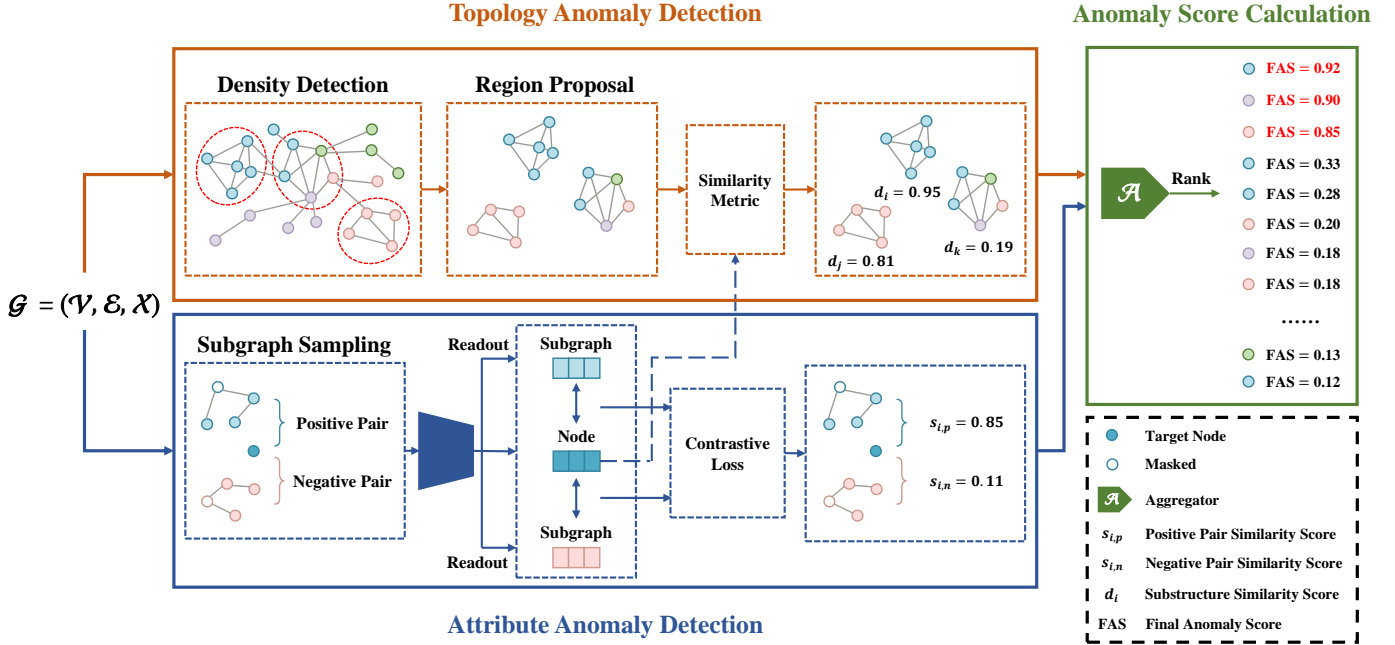


Figure 2: Overview of the GADMSL model. It consists of three modules: (1) Topology anomaly detection: We design a region proposal module to perceive high-density substructures as suspicious regions. The inner-node embedding similarities indicate how anomalous the substructures are; (2) Attribute anomaly detection: The target node forms a positive pair with its located subgraph and forms a negative pair with the irrelevant subgraph. After the contrastive learning network, the node embeddings are also used in topology anomaly detection; (3) Anomaly score calculation: We treat the reciprocal of substructure similarity score degree as the topology anomaly scores of its inner nodes and adopt a multi-scale substructure scoring strategy. The node attribute anomaly score is calculated by estimating the relationship between it and its contrastive subgraphs. Finally, the aggregator calculates the final anomaly score by fusing the attribute and topology anomaly scores of each node.

and network topology information to achieve powerful results. However, the traditional methods cannot excavate deep information, making it difficult to improve the performance continuously.

The emergence of graph neural networks (GNN) has dramatically improved the ability of the algorithms to extract the deep information of the attributed networks. They have been widely used in many fields [27]–[31]. It is natural to introduce GNN to graph anomaly detection. AAGNN [22], which is improved from the traditional anomaly detection algorithm, incorporates the one-class SVM algorithm into attributed networks to identify anomalous samples. Algorithms based on the self-supervised learning paradigm have also achieved great success. The generative self-supervised learning method DOMINANT [20] performs anomaly detection by calculating the differences between the attribute matrix, the adjacency matrix, and the original matrices after GCN reconstruction. Auxiliary attribute-based HCM [23] adopts a node-to-hop count pretext task that takes the predicted values of hop counts of nodes and first-order neighbors as node anomaly scores. CoLA [24] introduces the contrastive learning paradigm to ANAD for the first time, constructing node- and subgraph-level comparisons to identify anomalies by the differences between the node and contrastive subgraph attributes in positive and negative pairs. ANEMONE [32], SL-GAD [33], and Sub-CR [25] do further research on the basis of CoLA. Multi-scale strategies [34] have been proven effectively in other domains.

ANEMONE forms multi-scale contrastive with new node-level comparison and captures more anomalous information. SL-GAD adopts both contrastive learning and reconstruction patterns. Sub-CR works in a multi-view way with a global graph view generated by the diffusion model. However, most of these methods focus on digging the information of node attributes and pay less attention to the topological information.

### B. Graph Contrastive Learning

The primary purpose of graph neural network algorithms is to transform the attributes of nodes into low dimensions according to the needs of specific tasks. The expensive label-collection progress limits the supervised and semi-supervised learning algorithms. As an essential branch of the graph self-supervised paradigm, graph contrastive learning can compensate for the above problem to a certain extent by obtaining enough supervision information from ingenious-designed ingenious pretext tasks. Based on the contrastive scale [35], most graph contrastive learning methods can be divided into two leading mainstream. One is same-scale contrastive learning. GRACE [36] generates two comparison views by graph augmentation methods that bring the positive pair nodes in the view closer and push the negative pair nodes farther. After two graph views are generated, HeCO [37] is trained on the heterogeneous graph with encoders maximizing the mutual information of the same nodes in the views. To alleviate the burden of constructing negative pairs, BGRL [38] uses

Table I: Notation summary

Notations	Definitions
$\mathcal{G}$	An attributed network
$\mathbf{A} \in \mathbb{R}^{N \times N}$	The adjacency matrix of $\mathcal{G}$
$\mathbf{X} \in \mathbb{R}^{N \times D}$	The attribute matrix of $\mathcal{G}$
$v_i$	The $i^{th}$ node of $\mathcal{G}$
$\mathbf{x}_i \in \mathbb{R}^{1 \times D}$	The attribute vector of $v_i$
$\mathbf{H}^{(l)} \in \mathbb{R}^{N \times d}$	The hidden representation of the $l$ -th layer
$\mathbf{W}^{(l)} \in \mathbb{R}^{d \times d}$	The network parameters of the $l$ -th layer
$\mathbf{D} \in \mathbb{R}^{N \times N}$	The degree matrix of $\mathbf{A}$
$s_{i,p}^a$	The similarity between $v_i$ and subgraph in a positive pair
$y_{i,p}$	The ground-truth label of a positive pair
$C$	A substructure
$R^t$	The number of topology anomaly detection round
$R^a$	The number of attribute anomaly detection round
$S_i$	The final anomaly score of $v_i$

the Siamese network approach for model training. The other one is cross-scale contrastive learning. The pioneering work DGI [39] proposes to maximize the mutual information of node representation and graph level representation to obtain global information. After generating two views through data augmentation, MVGRL [40] maximizes the node representation in one view and the graph level representation in the other view. Therefore, we focus on using cross-scale contrastive learning, which provides a better solution to distill the representation of node attributes for ANAD tasks.

### III. THE PROPOSED METHOD

In this section, we will firstly define the main problem of ANAD formally. And the primary notations used throughout this paper are summarized in Table I. Then, we introduce the proposed framework, GADMSL.

#### A. Attributed Networks Anomaly Detection

An attributed network  $\mathcal{G} = (\mathcal{V}, \mathcal{E}, \mathbf{X})$  consists of: (1) the set of nodes  $\mathcal{V}$ , where  $|\mathcal{V}| = N$ ; (2) the set of edges  $\mathcal{E}$ , where  $|\mathcal{E}| = M$ ; (3) the node attributes matrix  $\mathbf{X} \in \mathbb{R}^{n \times d}$ , indicates the attribute values of nodes. In addition, the adjacency matrix  $\mathbf{A} \in \mathbb{R}^{n \times n}$  contains the topology information of the network, and  $\mathbf{A}_{ij} = 1$  represents there is an edge between node  $v_i$  and  $v_j$ , otherwise,  $\mathbf{A}_{ij} = 0$ .

In attributed networks anomaly detection, the model is trained to learn a function  $f$  that calculates the anomaly score  $S_i$  for node  $v_i$  in  $\mathcal{G}$ . The larger the anomaly score, the more likely the node is anomalous. It is worth noting that we conduct the attributed networks anomaly detection task strictly unsupervised in this paper.

#### B. Proposed Method

In the following subsection, we will introduce our method GADMSL. It consists of three main components. The first part is the topology anomaly detection module, which uses a density-based algorithm to perceive high-density substructures as suspicious regions. The anomaly degrees of the substructures are measured by estimating the inner-node similarities.

The second part is the attribute anomaly detection module, which forms a contrast of node- and subgraph-level to obtain node attribute anomaly degree. It should be pointed out that these two modules leverage both node attribute information and network topology information. The last one is the anomaly score calculation, which aggregates the anomalous information from the first two modules to obtain the final anomaly score for each node. Such two types of anomaly score calculations are performed under multi-round detection. In each detection, the former employs a multi-scale substructure scoring strategy, which takes into account the size of the substructure. The latter combines the effects of both positive and negative pairs.

1) *Topology Anomaly Detection*: Previous methods [24], [32], [33] constitute the positive and negative pairs in the contrastive network by random walk sampling. Nevertheless, the uncertain information caused by random walk is not always beneficial for learning the node-local topology information. When processing complex topology, the uncertainty may be counterproductive and result in unsatisfactory outcomes. We create a region proposal module to extract superior network topology information and suspicious substructures to overcome this deficiency. Afterward, we discriminate the anomalous substructures based on the similarities of inner-node attribute embeddings.

**Region Proposal Module.** According to the observation in the toy example, the topology anomalies most probably exist in the substructures with a mass of edges. To this end, we employ a density-based algorithm based on the  $k$ -core method [41] to discover the high-density substructures that may contain topology anomalies. In addition to this straightforward density-based algorithm, other more sophisticated algorithm strategies are also applicable under our substructure-aware framework as one of the potential directions in the future. Ultimately, these substructures  $\{C_0, \dots, C_j\}$  with possible anomalous nodes can be regarded as suspicious regions.

**Anomalous Substructure Discovery.** In reality, there are some scenarios where normal samples possess close connections between them, e.g., students in the same class follow each other on social media. Some suspicious regions have only normal nodes, while others contain normal nodes and topology anomalies. In light of this, we measure the anomaly degree of substructures by the node attribute information within them. It should be pointed out that the substructures with more significant differences in attributes between nodes have a higher anomaly possibility. Firstly, we compute the inner-node attribute similarities of the substructure. To obtain more accurate similarity, we utilize the embeddings of node attributes instead of the original attribute values. Specifically, we chose cosine distance as the similarity measurement:

$$d_{k,j} = \text{Similarity}(\mathbf{z}_k, \mathbf{z}_j) = \cos(\mathbf{z}_k, \mathbf{z}_j), \quad (1)$$

where  $\mathbf{z}_k$  and  $\mathbf{z}_j$  represents the embedding of node  $v_k$  and  $v_j$ .

After that, we regard the average value of the inner-node attribute similarities as the substructure similarity score. The

similarity score for each substructure can be defined as follows:

$$d_i = \frac{1}{n_i} \sum_{m=1}^{n_i} d_{k,j}^{(m)}, \quad (2)$$

where  $n_i$  is the numbers of the node pairs in the substructure  $\mathcal{C}_i$ . And node  $v_k$  and  $v_j$  belong to  $\mathcal{C}_i$ .

So far, it has not been solved how to obtain more qualified node embeddings for the similarity metric in Eq.(1). In addition, it is essential to detect attribute anomalies in ANAD. Hence, we introduce the graph contrastive learning scheme in attribute anomaly detection, which can acquire better node representations.

2) *Attribute Anomaly Detection*: The recent success of graph contrastive learning introduced in Section II-B has shown great potential to discern attribute abnormality. Inspired by this, we define contrastive instance pairs following [24]. Afterward, the node attribute anomaly degree is calculated by measuring the similarity between the embeddings of instance pairs. More importantly, GADMSL can learn better node representations served in the topology anomaly detection module.

**Subgraph Sampling.** The construction of positive and negative pairs is vital for contrastive learning. While there are multiple-scale contrasts, one of the most potent comparisons is the contrast of node and subgraph for ANAD. The supervision information from the subgraph includes both neighborhood attributes and topology. For the target node  $v_i$ , it forms a positive pair with the subgraph where it is located and forms a negative pair with the subgraph where another random node is located. To avoid the interaction between the node and subgraphs, the attribute values of the node are masked, i.e., all attribute values are set to 0.

There are many subgraph sampling methods, but we use a random walk-based algorithm [42]–[46] in this paper. Because it is practical and straightforward to implement. A generated subgraph is composed of a node and its neighborhoods.

**Contrastive Learning Network.** The contrastive learning network pulls the positive pairs and pushes the negative pairs in the latent space. In this process, the node representations are optimized. Firstly, we learn the representation of the subgraph through a GCN layer. The hidden layer representation of the subgraph in the positive pair can be defined as:

$$\mathbf{H}_{i,p}^{(l+1)} = \sigma \left( \tilde{\mathbf{D}}_{i,p}^{-\frac{1}{2}} \tilde{\mathbf{A}}_{i,p} \tilde{\mathbf{D}}_{i,p}^{-\frac{1}{2}} \mathbf{H}_{i,p}^{(l)} \mathbf{W}^{(l)} \right), \quad (3)$$

where  $\mathbf{H}_{i,p}^{(l+1)}$  and  $\mathbf{H}_{i,p}^{(l)}$  denote the hidden representation of the  $(l+1)$ -th and  $l$ -th layer,  $\tilde{\mathbf{D}}_{i,p}^{-\frac{1}{2}} \tilde{\mathbf{A}}_{i,p} \tilde{\mathbf{D}}_{i,p}^{-\frac{1}{2}}$  is the normalization of the adjacency matrix,  $\mathbf{W}^{(l)}$  denotes the network parameters,  $\sigma(\cdot)$  is activation function ReLU here. The subgraph in the negative pair can also be defined like this.

After GCN, we manage to define a *Readout* function, which converts the embedding of the subgraph  $\mathbf{Z}_{i,p}$  to the same shape as the target node. In practice, we choose average to achieve *Readout*:

$$\mathbf{z}_{i,p} = \text{Readout}(\mathbf{Z}_{i,p}) = \sum_{j=1}^{n_i} \frac{(\mathbf{Z}_{i,p})_j}{n_i}, \quad (4)$$

where  $n_i$  denotes the number of nodes within the subgraph,  $(\mathbf{Z}_{i,p})_j$  denotes the  $j$ -th row of  $\mathbf{Z}_{i,p}$ , and  $\mathbf{z}_{i,p}$  is the final representation of the subgraph.

Then, we need to encode the attribute of the target node into the same embedding space as subgraphs. The embedding of the target node can be acquired by using the model parameters of GCN:

$$\mathbf{h}_i^{(l+1)} = \sigma \left( \mathbf{h}_i^{(l)} \mathbf{W}^{(l)} \right), \quad (5)$$

where  $\mathbf{h}_i^{(l+1)}$  and  $\mathbf{h}_i^{(l)}$  denote the hidden representation of the  $(l+1)$ -th and  $l$ -th layer,  $\mathbf{W}^{(l)}$  denotes the network parameters,  $\sigma(\cdot)$  is ReLU here. The last two are both shared with GCN.  $\mathbf{z}_i$  is the final representation of the target node.

We utilize a bilinear model to tease out the relationship between the target node and contrastive subgraphs, i.e., the similarity:

$$s_{i,p}^a = \text{Bilinear}(\mathbf{z}_{i,p}, \mathbf{z}_i) = \text{sigmoid}(\mathbf{z}_{i,p} \mathbf{W}_p \mathbf{z}_i^\top), \quad (6)$$

where  $\mathbf{W}_p$  denotes the parameter matrix, and  $\text{sigmoid}(\cdot)$  is the logistic sigmoid function.

According to the characteristics of the ANAD task, we decide to apply the binary cross-entropy loss [39] as the objective function of the module. It can be expressed as follows:

$$\mathcal{L} = - \sum_{i=1}^N (y_{i,p} \log(s_{i,p}^a) + (1 - y_{i,p}) \log(1 - s_{i,p}^a)), \quad (7)$$

where  $y_{i,p}$  is the ground-truth label of the positive pair, which is equal to 1. The expression of the negative pair can also be defined like these, but the ground-truth label  $y_{i,n}$  is equal to 0.

3) *Anomaly Score Calculation: Topology Anomaly Score.* Since the inner-node embedding similarities are negatively correlated with the anomaly degree of the substructure, the reciprocal of the substructure similarity score is naturally used to represent its anomaly degree. Then we treat the substructure anomaly score  $s_i^t$  as the topology anomaly score of its inner nodes. If a node is not in any previously detected substructure, its topology anomaly score is 0. We calculate the topology anomaly score for each node in the substructure:

$$s_i^t = \frac{1}{d_i}. \quad (8)$$

Owing to the uncertain substructure size in topology anomaly detection, multi-round detection is needed until the largest high-density substructure is observed. To avoid unnecessary calculations, we set  $k$  to the average degree of the nodes in the graph and start the density-based algorithm. And we end the algorithm when it finds the largest substructure. In the meantime, we adopt a new multi-scale substructure scoring strategy. We argue that nodes in substructures of different sizes should be given different topology anomaly scores. It is a natural idea that nodes in larger substructures should be given larger topology anomaly scores. In practice, we adopt the number of nodes in substructure to measure this impact.

Therefore, we finally average the anomaly scores from multi-round detection to determine the topology anomaly score for each node. So the final topology anomaly score of the target node can be defined as follows:

$$s_i^t = \frac{1}{R^t} \sum_{r=1}^{R^t} |C_i| s_i^{t(r)}, \quad (9)$$

where  $|C_i|$  indicates the number of the node in the substructure  $C_i$ , and  $R^t$  is the number of topology anomaly detection round.  $s_i^t$  denotes the final topology anomaly score of the target node  $v_i$ .

**Attribute Anomaly Score.** The attribute anomaly detection module obtains the similarities between the embeddings of each target node and contrastive subgraphs. We calculate the node attribute anomaly score according to the similarities information. For a normal node, its embedding should be similar to the subgraph in the positive pair, i.e.,  $s_{i,p}$  close to 1. On the contrary, it is dissimilar to the subgraph in the negative pair, i.e.,  $s_{i,n}$  close to 0. For an anomalous node, its embedding should be dissimilar to the subgraphs in both positive and negative pairs, i.e.,  $s_{i,p}$  and  $s_{i,n}$  both close to 0. In some extreme instances, the anomalous node is instead similar to the subgraph in the negative pair. Therefore, we define the attribute anomaly score of the target node as follows:

$$s_i^a = s_{i,n}^a - s_{i,p}^a. \quad (10)$$

Due to the randomness of the subgraph sampling method, it cannot reflect all the attribute information of the node neighborhoods in a single sampling. Thus, we perform multi-round detection and construct multiple groups of positive and negative pairs. Then the final attribute anomaly score of the target node is expressed as follows:

$$s_i^a = \frac{1}{R^a} \sum_{r=1}^{R^a} s_i^{a(r)}, \quad (11)$$

where  $s_i^a$  denotes the final attribute anomaly score of the target node  $v_i$ , and  $R^a$  is the number of attribute anomaly detection round.

**Final Anomaly Score.** Once the attribute anomaly score and topology anomaly score for each node are determined, we design an aggregator to fuse them. Firstly, each kind of score is normalized to unify its magnitudes. Then the aggregator sums the two scores according to the weight and obtains the final anomaly score for each node:

$$S_i = (1 - \alpha) s_i^t + \alpha s_i^a, \quad (12)$$

where  $\alpha \in [0, 1]$  is a trade-off parameter to balance the importance between two scores.

In general, the overall procedures of GADMSL are shown in Algorithm 1.

#### IV. EXPERIMENT

To verify the effectiveness of GADMSL, in this section, we conduct experiments on six benchmark datasets and evaluate the model through three metrics.

---

#### Algorithm 1 The proposed GADMSL.

---

**Input:** An attributed network  $\mathcal{G} = (\mathcal{V}, \mathcal{E}, \mathbf{X})$ ; Number of training epochs  $E$ ; Batch size  $B$ .

**Output:** Anomaly score function  $f$ .

```

1: // Topology anomaly detection
2: Calculate the average degree  $D$  of nodes in graph.
3: for  $k = D$  to  $k_{max}$  do
4:   Detect high-density substructures  $\{C_0, \dots, C_j\}$ .
5:   for  $C_i$  do
6:     Measure the inner-node embedding similarities of  $C_i$  via Eq.(1).
7:     Calculate the similarity score for each substructure via Eq.(2).
8:   end for
9: end for
10: // Attribute anomaly detection
11: for  $e = 1$  to  $E$  do
12:    $\mathcal{V}$  is divided into batches with size  $B$  by random.
13:   for  $v_i \in B$  do
14:     Form the positive and negative pairs by random walk sampling.
15:     Estimate the similarity scores for the embeddings of target node and two subgraphs in the positive and negative pair via Eq.(6).
16:     Calculate the loss  $\mathcal{L}$  via Eq.(7).
17:     Back propagation and update trainable parameters.
18:   end for
19: end for
20: // Anomaly score calculation
21: By multiple round detection, calculate the final anomaly score for each node via Eq.(8), (9), (10), (11), and (12).

```

---

#### A. Experimental Settings

1) *Datasets:* We perform experiments on six datasets commonly used in ANAD. The details of each dataset are presented in Table II. They are Cora [47], CiteSeer [47], DBLP [48], Citation [48], ACM [48], and PubMed [47]. DBLP is an author network. There is an edge between two authors if they are coauthor relationship. The others are publication network datasets, which are composed of scientific publications. Each paper is regarded as a node. The citation relations form the edges in the network.

Table II: The statistics of datasets.

Datasets	Nodes	Edges	Attributes	Anomalies
<b>Cora</b>	2708	5429	1433	150
<b>CiteSeer</b>	3327	4732	3703	150
<b>DBLP</b>	5484	8117	6775	300
<b>Citation</b>	8935	15098	6775	450
<b>ACM</b>	9360	15556	6775	450
<b>PubMed</b>	19717	44338	500	600

2) *Anomaly Injection:* Since the above six datasets are commonly attributed network datasets, they are usually considered to have no anomalous nodes. Therefore, we need to inject anomalous nodes into these datasets for the experiment to work correctly. Following the previous literature [12]–[14], we inject both topology and attribute anomalies into the datasets. Considering the balance, such two types of anomalies have the same number in each dataset.

**Topology anomaly injection.** Topology anomalies are mainly generated by perturbing the topology of the attributed networks. If many nodes in the dataset with dissimilar attributes are much more closely connected than the average, this can be considered a typical anomalous situation [12], [13]. Specifically, we randomly select  $m$  nodes that make them fully connected. The number  $m$  is set to 15 in practice. The number of node sets is 5, 5, 10, 15, 15, and 20 on Cora, CiteSeer, DBLP, Citation ACM, and PubMed.

**Attribute anomaly injection.** Attribute anomalies are mainly generated by perturbing the attribute values of nodes. Using the method proposed in the literature [14], attribute anomalies are generated by modifying node attribute values. Firstly, we randomly select a node  $v_i$  and another  $n$  nodes. The number  $n$  is usually 50. Then we calculate the Euclidean distance between  $v_i$  and each of the  $n$  nodes. Finally, the attribute values of  $v_i$  are changed to be the same as that of node  $v_j$ , which have the largest Euclidean distance. The number of attribute anomalies is 75, 75, 150, 225, 225, and 300 on each dataset.

3) *Baselines:* We select eight well-known ANAD algorithms to compare with our proposed framework, GADMSL. They are LOF<sup>1</sup> [15], ANOMALOUS<sup>2</sup> [19], DOMINANT<sup>3</sup> [20], CoLA<sup>4</sup> [24], ANEMONE<sup>5</sup> [32], SLGAD<sup>6</sup> [33], HCM<sup>7</sup> [23] and Sub-CR<sup>8</sup> [25]. The first two are non-deep methods, and the last six are deep methods. Following the operation of CoLA, the datasets are first pre-processed before running ANOMALOUS. Specifically, the attributes dimension of nodes is reduced to 30 by PCA.

4) *Evaluation Metric:* Our experiments employ three common metrics to evaluate the model comprehensively.

**AUC-ROC.** The ROC curve is a plot of true positive rate against false positive rate according to the ground truth and the anomaly scores of the nodes. AUC value is the area under the ROC curve. A higher value means the score function assigns a higher score to the randomly chosen anomalous sample than a normal sample.

**AUC-PR.** The PR curve is a plot of precision against recall according to the ground truth and the anomaly scores of the nodes. AUPRC value is the area under the PR curve, reflecting the performance of the positive samples. In practice, we use the method of calculating the average accuracy to obtain AUPRC value [49].

**Precision@K.** It indicates the proportion of true-positive samples among the top  $k$  samples with the largest anomaly scores. The value of Precision@K ranges from 0 to 1, and close to 1 means the model performs better.

5) *Parameter Settings:* In the attribute anomaly detection module, we set the size of subgraphs in positive pairs and negative pairs to be 4. In the meantime, the basic network

model (GCN) is one layer, and the latent embedding dimension is 64 on all datasets. The learning rate of the model for Cora, CiteSeer, DBLP, Citation, ACM, and PubMed is 0.003, 0.003, 0.0005, 0.001, 0.0005, and 0.001. To get better performance, the number of training epochs on Cora, CiteSeer, and PubMed is 100. It is set to 400 on DBLP, Citation, and ACM.

6) *Computing Infrastructures:* Except for ANOMALOUS, the experiments of other models run on the PyTorch 1.10.2 platform using an Intel (R) Core (TM) i9-10850K CPU (3.60GHz), 64GB RAM, and an NVIDIA GeForce RTX 3070 8GB GPU. The experiments of ANOMALOUS run on MATLAB R2020b platform using the same machine.

## B. Experimental Results

The ROC curves of these nine models on these five datasets are shown in Figure 3. The specific AUC values and AUPRC values are shown in Table III. Meanwhile, the Precision@K of total anomaly and topology anomaly line diagrams are shown in Figure 4. Through comparison, we can draw the conclusions as follows:

1) *AUC and AUPRC results:* As shown in Table III, we observe that GADMSL has a stronger ability to distinguish anomalous nodes from normal nodes than other models. In particular, GADMSL attains a remarkable AUC gain of **2.46%**, **0.62%**, **1.85%**, **7.30%**, **2.92%** and **0.52%** on Cora, CiteSeer, DBLP, Citation, ACM, and PubMed, respectively. At the same time, the AUPRC results reflect that GADMSL makes a remarkable improvement in the positive sample detection compared with its competitors on most datasets, and it obtains about **17.46%** AUPRC increment on the ACM dataset. These indicate that GADMSL has a more comprehensive performance and can adapt to the different needs of various scenarios. It is worth noting that the well-design topology anomaly detection module brings about **2.19%-15.29%** AUC and **11.97%-34.32%** AUPRC gains when compared with the pioneering baseline CoLA.

Figure 3 offers an intuitive illustration that the under-curve areas of the deep methods are significantly larger than most non-deep methods, and the contrastive learning-based methods work best among the deep methods. This indicates that deep methods, especially contrastive learning-based methods, can learn more effective embeddings of node attribute values than non-deep methods for the ANAD task.

2) *Precision@K results:* For a more comprehensive evaluation, we also report Precision@K on the six datasets in Figure 4. For each dataset, the odd columns are Precision@K results reflecting the proportion of true total anomalies, which contains both attribute and topology anomalies, in its top  $k$  ranked nodes. The even columns are Precision@K measuring the proportion of veritable topology anomalies in its top  $k$  anomaly scores. As suggested by results in Figure 4, GADMSL achieves best or comparable results in odd column subfigures. It is noticeable that GADMSL brings tangible Precision@K improvement to the competitors except on Citation in even column subfigures. These phenomena verify the effectiveness of our novel substructure-based paradigm on topology anomaly detection.

<sup>1</sup> <https://github.com/damjankuznar/pylof>

<sup>2</sup> <https://github.com/zpeng27/ANOMALOUS>

<sup>3</sup> [https://github.com/kaize0409/GCN\\_AnomalyDetection\\_pytorch](https://github.com/kaize0409/GCN_AnomalyDetection_pytorch)

<sup>4</sup> <https://github.com/GRAND-Lab/CoLA>

<sup>5</sup> <https://github.com/GRAND-Lab/ANEMONE>

<sup>6</sup> <https://github.com/KimMeen/SL-GAD>

<sup>7</sup> <https://github.com/Juintin/GraphAnomalyDetection>

<sup>8</sup> <https://github.com/Zjer12/Sub>

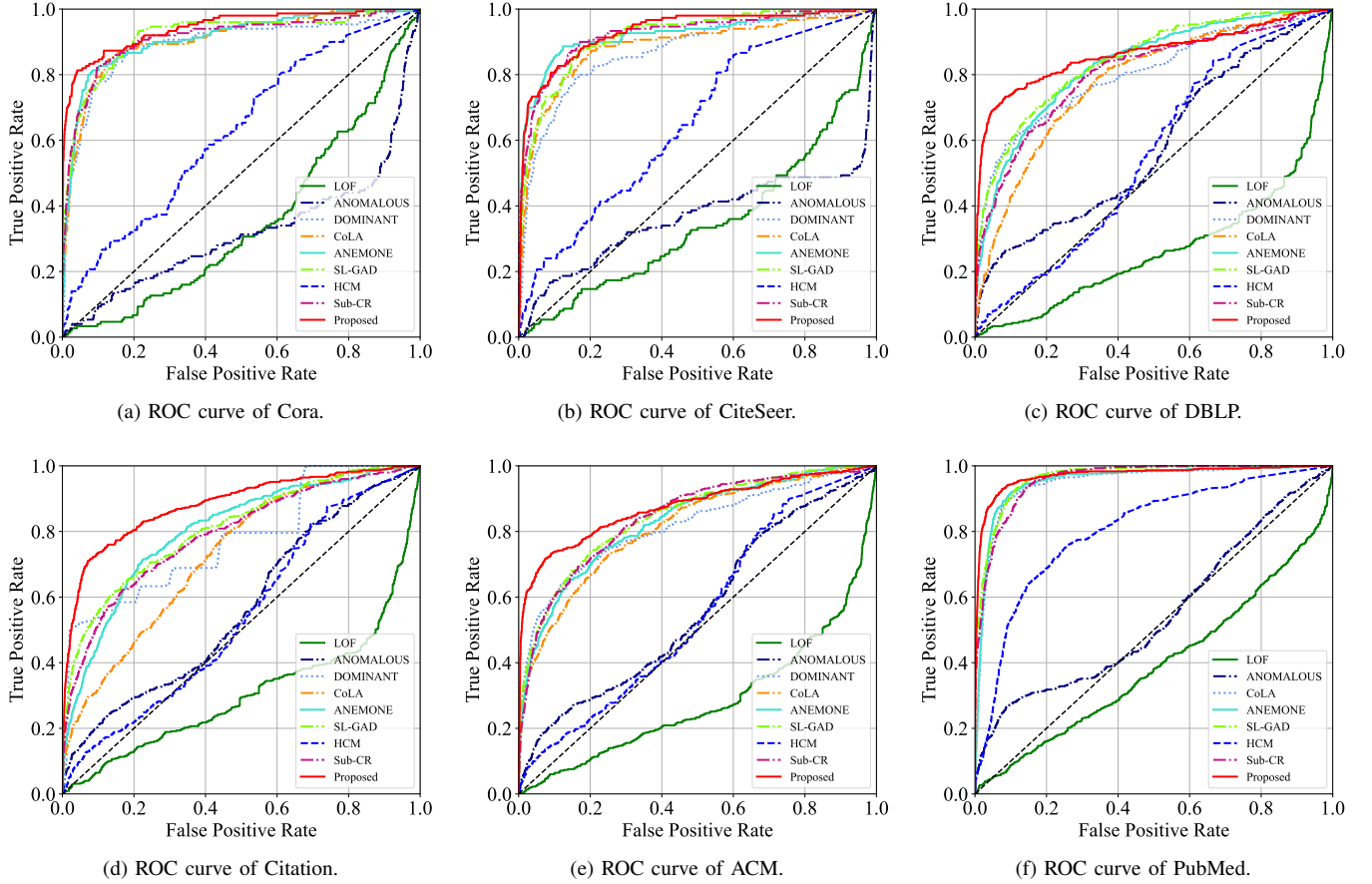


Figure 3: ROC curves comparison on six benchmark datasets. The area under the curve is larger, the anomaly detection performance is better. The black dotted lines are the "random line", indicating the performance under random guessing.

Table III: Performance comparison for AUC and AUPRC. OOM indicates the issue Out-Of-Memory happens during training. The bold and underline values indicate the best and runner-up results, respectively.

Methods	Cora		CiteSeer		DBLP		Citation		ACM		PubMed	
	AUC	AUPRC	AUC	AUPRC	AUC	AUPRC	AUC	AUPRC	AUC	AUPRC	AUC	AUPRC
LOF	0.3538	0.0411	0.3484	0.0339	0.2694	0.0363	0.3059	0.0360	0.2843	0.0321	0.3934	0.0256
ANOMALOUS	0.3198	0.0432	0.3669	0.0445	0.5846	0.1187	0.5656	0.0829	0.5626	0.0764	0.5450	0.0688
DOMINANT	0.8929	0.4474	0.8718	0.3308	0.8034	0.3738	0.7748	0.2773	0.8152	0.3553	OOM	OOM
CoLA	0.9065	0.5065	0.8863	0.4303	0.7824	0.2051	0.7296	0.1928	0.8127	0.3214	0.9493	0.4169
ANEMONE	0.9122	0.5320	0.9227	<b>0.6281</b>	0.8322	0.3271	0.8028	0.2578	0.8300	0.3539	0.9552	0.4274
SL-GAD	<u>0.9192</u>	<u>0.6022</u>	0.9177	0.5263	<u>0.8461</u>	<u>0.4061</u>	<u>0.8095</u>	<u>0.3473</u>	<u>0.8450</u>	<u>0.3886</u>	<u>0.9660</u>	<u>0.6351</u>
HCM	0.6276	0.1090	0.6502	0.0934	0.5572	0.0695	0.5414	0.0612	0.5507	0.0674	0.8065	0.1400
Sub-CR	0.9133	0.5922	<u>0.9248</u>	<u>0.6083</u>	0.8061	0.3336	0.7903	0.2968	0.8428	0.3469	0.9594	0.5854
<b>Proposed</b>	<b>0.9438</b>	<b>0.7750</b>	<b>0.9310</b>	0.5500	<b>0.8646</b>	<b>0.5483</b>	<b>0.8825</b>	<b>0.4924</b>	<b>0.8742</b>	<b>0.5632</b>	<b>0.9712</b>	<b>0.7287</b>

### C. Ablation Study and Parameter Analysis

In this section, we explore the effect of the score-fusion and node representation acquisition strategies on the model performance. Besides, we analyze the coefficient  $\alpha$  influence on the score-fusion strategy.

1) *Analysis of the fusion strategy for topology and attribute anomaly scores*: After gathering equally important topology and attribute anomaly scores, we analyze the fusion strategies to get final anomaly scores. To boost the performance, we explore three different combination strategies: (1) Max: We choose the largest value to represent the node anomaly de-

gree; (2) Sum: We sum the two scores directly; (3) Weight: The scores are summed by weight. As shown in Table IV, GADMSL adopts the weight fusion strategy, which is not always the best but the most robust choice.

2) *Analysis of the node representations learned by GADMSL*: In the topology anomaly module, the inner-node embedding similarities are highly correlated with the anomalous degree of the substructure. Hence, how to enjoy better node representations becomes a vital problem. We compare



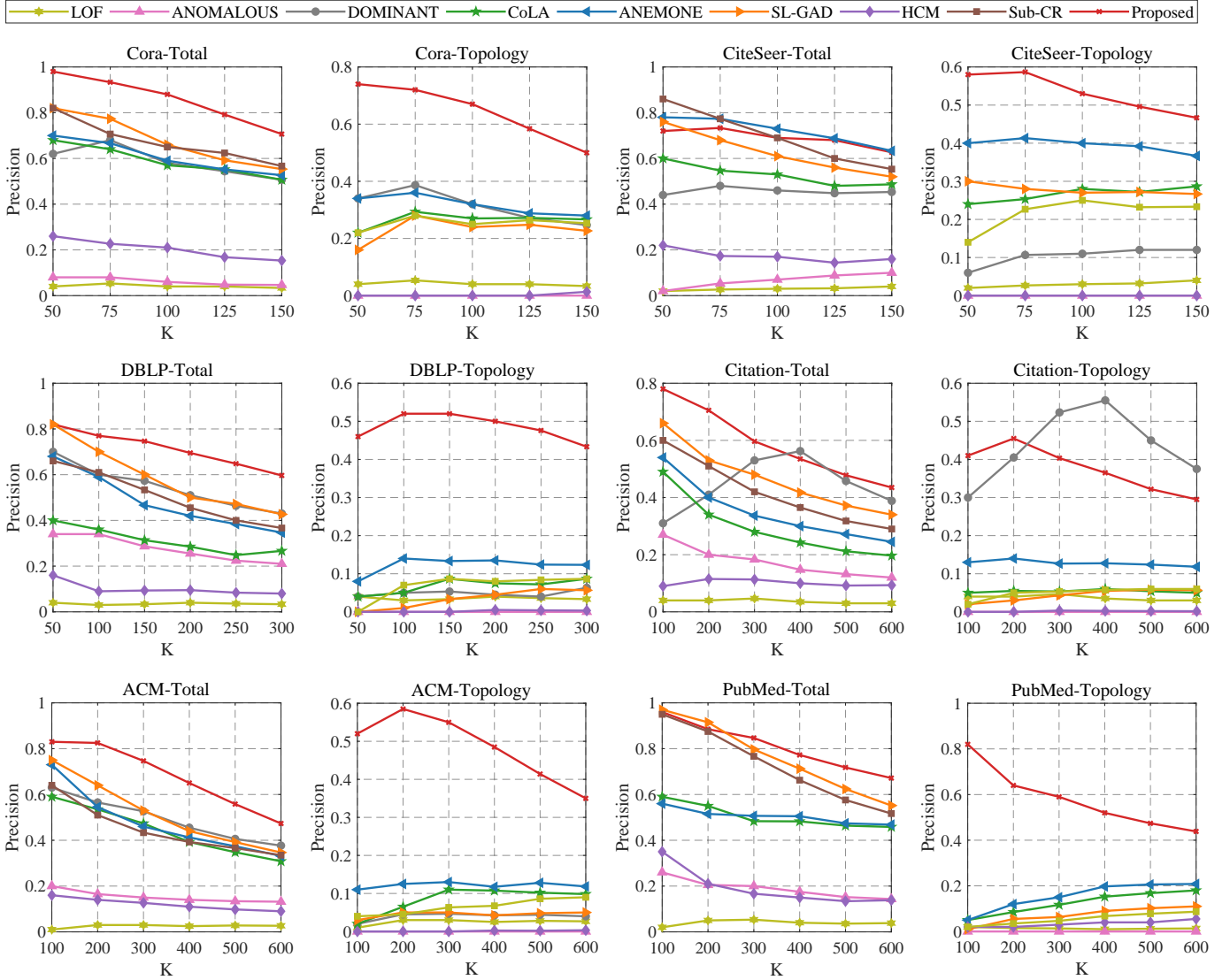


Figure 4: Performance comparison results w.r.t. Precision@K of total anomaly and topology anomaly on four benchmark datasets.

Table IV: Ablation analysis for the fusion method of topology and attribute anomaly scores w.r.t. AUC values. The bold values indicate the best results.

	Cora	CiteSeer	DBLP	Citation	ACM	PubMed
Max	<b>0.9448</b>	0.9116	0.8539	0.8527	0.8645	0.9408
Sum	0.9280	0.8922	0.8356	0.8421	0.8391	0.9266
Weight	0.9438	<b>0.9310</b>	<b>0.8646</b>	<b>0.8825</b>	<b>0.8742</b>	<b>0.9712</b>

the performance of using raw node attributes with node embeddings from the contrastive network. Table V shows that the contrastive network learns more effective node representations for topology anomaly detection, further enhancing the ANAD performance.

3) *Analysis of coefficient  $\alpha$* : As shown in Figure 5, we vary the coefficient  $\alpha$  from 0 to 1.0 and obtain its effect

Table V: Ablation analysis for the method of obtaining node representations w.r.t. AUC values. The bold values indicate the best results.

	Cora	CiteSeer	DBLP	Citation	ACM	PubMed
Raw	0.9270	0.8992	0.8623	0.8721	0.8682	0.9663
Contrastive	<b>0.9437</b>	<b>0.9310</b>	<b>0.8646</b>	<b>0.8825</b>	<b>0.8742</b>	<b>0.9712</b>

on the AUC value. Finally, we adopt  $\alpha$  is equal to 0.80 on all datasets. We note that the lines show an upward trend followed by a downward trend. The performance on  $\alpha = 0$  or  $\alpha = 1$  is significantly lower when  $\alpha$  is equal to another value. This reflects that using the topology and attribute anomaly module concurrently greatly improves the detection ability of the model compared with only one.

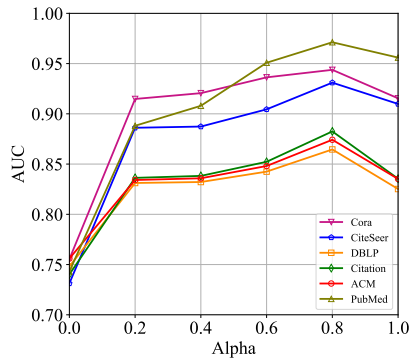


Figure 5: Trade-off parameter  $\alpha$  w.r.t. AUC values.

## V. CONCLUSION

In this paper, we propose a novel substructure-aware attributed networks anomaly detection framework termed GADMSL. Different from existing works, we design a new topology anomaly detection module. We use a density-based algorithm to detect high-density substructures as the region proposed. Then, the inner-node embedding similarities of substructures are measured to find out the ones that contain topology anomalies. For this purpose, we introduce a graph contrastive learning method to obtain better embeddings of node attributes and to detect attribute anomalies. The experiments demonstrate that GADMSL makes a great improvement on attributed networks anomaly detection. In future work, we will improve the algorithm to meet the needs of datasets with more nodes and more complex network topology. At the same time, we will continue to explore how to better aggregate the attribute and topology anomaly scores of nodes to avoid information loss.

## REFERENCES

- [1] P. Cui, X. Wang, J. Pei, and W. Zhu, "A survey on network embedding," *IEEE transactions on knowledge and data engineering*, vol. 31, no. 5, pp. 833–852, 2018.
- [2] Z. Wu, S. Pan, F. Chen, G. Long, C. Zhang, and S. Y. Philip, "A comprehensive survey on graph neural networks," *IEEE transactions on neural networks and learning systems*, vol. 32, no. 1, pp. 4–24, 2020.
- [3] S. Zhu, S. Pan, C. Zhou, J. Wu, Y. Cao, and B. Wang, "Graph geometry interaction learning," *Advances in Neural Information Processing Systems*, vol. 33, pp. 7548–7558, 2020.
- [4] F. Liu, S. Xue, J. Wu, C. Zhou, W. Hu, C. Paris, S. Nepal, J. Yang, and P. S. Yu, "Deep learning for community detection: progress, challenges and opportunities," in *Proceedings of the Twenty-Ninth International Conference on Artificial Intelligence*, 2021, pp. 4981–4987.
- [5] X. Su, S. Xue, F. Liu, J. Wu, J. Yang, C. Zhou, W. Hu, C. Paris, S. Nepal, D. Jin *et al.*, "A comprehensive survey on community detection with deep learning," *IEEE Transactions on Neural Networks and Learning Systems*, 2022.
- [6] L. Akoglu, H. Tong, and D. Koutra, "Graph based anomaly detection and description: a survey," *Data mining and knowledge discovery*, vol. 29, no. 3, pp. 626–688, 2015.
- [7] G. Zhang, Z. Li, J. Huang, J. Wu, C. Zhou, J. Yang, and J. Gao, "efraudcom: An e-commerce fraud detection system via competitive graph neural networks," *ACM Transactions on Information Systems (TOIS)*, vol. 40, no. 3, pp. 1–29, 2022.
- [8] S. Rao, A. K. Verma, and T. Bhatia, "A review on social spam detection: Challenges, open issues, and future directions," *Expert Systems with Applications*, vol. 186, p. 115742, 2021.
- [9] M. Mongiovi, P. Bogdanov, R. Ranca, E. E. Papalexakis, C. Faloutsos, and A. K. Singh, "NetSpot: Spotting significant anomalous regions on dynamic networks," in *Proceedings of the 2013 SIAM international conference on data mining*. SIAM, 2013, pp. 28–36.
- [10] Y. Boshmaf, K. Beznosov, and M. Ripeanu, "Graph-based sybil detection in social and information systems," in *2013 IEEE/ACM International Conference on Advances in Social Networks Analysis and Mining (ASONAM 2013)*. IEEE, 2013, pp. 466–473.
- [11] X. Ma, J. Wu, S. Xue, J. Yang, C. Zhou, Q. Z. Sheng, H. Xiong, and L. Akoglu, "A comprehensive survey on graph anomaly detection with deep learning," *IEEE Transactions on Knowledge and Data Engineering*, 2021.
- [12] K. Ding, J. Li, and H. Liu, "Interactive anomaly detection on attributed networks," in *Proceedings of the twelfth international conference on web search and data mining*, 2019, pp. 357–365.
- [13] D. B. Skillicorn, "Detecting anomalies in graphs," in *2007 IEEE Intelligence and Security Informatics*. IEEE, 2007, pp. 209–216.
- [14] X. Song, M. Wu, C. Jermaine, and S. Ranka, "Conditional anomaly detection," *IEEE Transactions on knowledge and Data Engineering*, vol. 19, no. 5, pp. 631–645, 2007.
- [15] M. M. Breunig, H.-P. Kriegel, R. T. Ng, and J. Sander, "Lof: identifying density-based local outliers," in *Proceedings of the 2000 ACM SIGMOD international conference on Management of data*, 2000, pp. 93–104.
- [16] X. Xu, N. Yuruk, Z. Feng, and T. A. Schweiger, "Scan: a structural clustering algorithm for networks," in *Proceedings of the 13th ACM SIGKDD international conference on Knowledge discovery and data mining*, 2007, pp. 824–833.
- [17] B. Perozzi and L. Akoglu, "Scalable anomaly ranking of attributed neighborhoods," in *Proceedings of the 2016 SIAM International Conference on Data Mining*. SIAM, 2016, pp. 207–215.
- [18] J. Li, H. Dani, X. Hu, and H. Liu, "Radar: Residual analysis for anomaly detection in attributed networks," in *IJCAI*, 2017, pp. 2152–2158.
- [19] Z. Peng, M. Luo, J. Li, H. Liu, and Q. Zheng, "Anomalous: A joint modeling approach for anomaly detection on attributed networks," in *IJCAI*, 2018, pp. 3513–3519.
- [20] K. Ding, J. Li, R. Bhanushali, and H. Liu, "Deep anomaly detection on attributed networks," in *Proceedings of the 2019 SIAM International Conference on Data Mining*. SIAM, 2019, pp. 594–602.
- [21] K. Ding, X. Shan, and H. Liu, "Towards anomaly-resistant graph neural networks via reinforcement learning," in *Proceedings of the 30th ACM International Conference on Information & Knowledge Management*, 2021, pp. 2979–2983.
- [22] S. Zhou, Q. Tan, Z. Xu, X. Huang, and F.-I. Chung, "Subtractive aggregation for attributed network anomaly detection," in *Proceedings of the 30th ACM International Conference on Information & Knowledge Management*, 2021, pp. 3672–3676.
- [23] T. Huang, Y. Pei, V. Menkovski, and M. Pechenizkiy, "Hop-count based self-supervised anomaly detection on attributed networks," *arXiv preprint arXiv:2104.07917*, 2021.
- [24] Y. Liu, Z. Li, S. Pan, C. Gong, C. Zhou, and G. Karypis, "Anomaly detection on attributed networks via contrastive self-supervised learning," *IEEE transactions on neural networks and learning systems*, 2021.
- [25] J. Zhang, S. Wang, and S. Chen, "Reconstruction enhanced multi-view contrastive learning for anomaly detection on attributed networks," *arXiv preprint arXiv:2205.04816*, 2022.
- [26] J. M. Lobo, A. Jiménez-Valverde, and R. Real, "Auc: a misleading measure of the performance of predictive distribution models," *Global ecology and Biogeography*, vol. 17, no. 2, pp. 145–151, 2008.
- [27] X. He, K. Deng, X. Wang, Y. Li, Y. Zhang, and M. Wang, "Lightgcn: Simplifying and powering graph convolution network for recommendation," in *Proceedings of the 43rd International ACM SIGIR conference on research and development in Information Retrieval*, 2020, pp. 639–648.
- [28] L. Chen, L. Wu, R. Hong, K. Zhang, and M. Wang, "Revisiting graph based collaborative filtering: A linear residual graph convolutional network approach," in *Proceedings of the AAAI conference on artificial intelligence*, vol. 34, no. 01, 2020, pp. 27–34.
- [29] L. Wu, P. Sun, R. Hong, Y. Fu, X. Wang, and M. Wang, "Socialgcn: An efficient graph convolutional network based model for social recommendation," *arXiv preprint arXiv:1811.02815*, 2018.
- [30] J. Liu, Z.-J. Zha, R. Hong, M. Wang, and Y. Zhang, "Deep adversarial graph attention convolution network for text-based person search," in *Proceedings of the 27th ACM International Conference on Multimedia*, 2019, pp. 665–673.
- [31] J. Shuai, K. Zhang, L. Wu, P. Sun, R. Hong, M. Wang, and Y. Li, "A review-aware graph contrastive learning framework for recommendation," *arXiv preprint arXiv:2204.12063*, 2022.

- [32] M. Jin, Y. Liu, Y. Zheng, L. Chi, Y.-F. Li, and S. Pan, “Anemone: Graph anomaly detection with multi-scale contrastive learning,” in *Proceedings of the 30th ACM International Conference on Information & Knowledge Management*, 2021, pp. 3122–3126.
- [33] Y. Zheng, M. Jin, Y. Liu, L. Chi, K. T. Phan, and Y.-P. P. Chen, “Generative and contrastive self-supervised learning for graph anomaly detection,” *IEEE Transactions on Knowledge and Data Engineering*, 2021.
- [34] Y. Wang, J. Peng, H. Wang, and M. Wang, “Progressive learning with multi-scale attention network for cross-domain vehicle re-identification,” *Science China Information Sciences*, vol. 65, no. 6, pp. 1–15, 2022.
- [35] Y. Liu, M. Jin, S. Pan, C. Zhou, Y. Zheng, F. Xia, and P. Yu, “Graph self-supervised learning: A survey,” *IEEE Transactions on Knowledge and Data Engineering*, 2022.
- [36] Y. Zhu, Y. Xu, F. Yu, Q. Liu, S. Wu, and L. Wang, “Deep graph contrastive representation learning,” *arXiv preprint arXiv:2006.04131*, 2020.
- [37] X. Wang, N. Liu, H. Han, and C. Shi, “Self-supervised heterogeneous graph neural network with co-contrastive learning,” in *Proceedings of the 27th ACM SIGKDD Conference on Knowledge Discovery & Data Mining*, 2021, pp. 1726–1736.
- [38] S. Thakoor, C. Tallec, M. G. Azar, R. Munos, P. Veličković, and M. Valko, “Bootstrapped representation learning on graphs,” in *ICLR 2021 Workshop on Geometrical and Topological Representation Learning*, 2021.
- [39] P. Veličković, W. Fedus, W. L. Hamilton, P. Liò, Y. Bengio, and R. D. Hjelm, “Deep graph infomax,” *ICLR (Poster)*, vol. 2, no. 3, p. 4, 2019.
- [40] K. Hassani and A. H. Khasahmadi, “Contrastive multi-view representation learning on graphs,” in *International Conference on Machine Learning*. PMLR, 2020, pp. 4116–4126.
- [41] V. Batagelj and M. Zaversnik, “An  $o(m)$  algorithm for cores decomposition of networks,” *arXiv preprint cs/0310049*, 2003.
- [42] H. Tong, C. Faloutsos, and J.-Y. Pan, “Fast random walk with restart and its applications,” in *Sixth international conference on data mining (ICDM’06)*. IEEE, 2006, pp. 613–622.
- [43] B. Perozzi, R. Al-Rfou, and S. Skiena, “Deepwalk: Online learning of social representations,” in *Proceedings of the 20th ACM SIGKDD international conference on Knowledge discovery and data mining*, 2014, pp. 701–710.
- [44] J. Qiu, Q. Chen, Y. Dong, J. Zhang, H. Yang, M. Ding, K. Wang, and J. Tang, “Gcc: Graph contrastive coding for graph neural network pre-training,” in *Proceedings of the 26th ACM SIGKDD International Conference on Knowledge Discovery & Data Mining*, 2020, pp. 1150–1160.
- [45] Y. Wang, W. Zhang, L. Wu, X. Lin, and X. Zhao, “Unsupervised metric fusion over multiview data by graph random walk-based cross-view diffusion,” *IEEE transactions on neural networks and learning systems*, vol. 28, no. 1, pp. 57–70, 2015.
- [46] Y. Wang, X. Lin, and Q. Zhang, “Towards metric fusion on multi-view data: a cross-view based graph random walk approach,” in *Proceedings of the 22nd ACM international conference on Information & Knowledge Management*, 2013, pp. 805–810.
- [47] P. Sen, G. Namata, M. Bilgic, L. Getoor, B. Galligher, and T. Eliassi-Rad, “Collective classification in network data,” *AI magazine*, vol. 29, no. 3, pp. 93–93, 2008.
- [48] X. Yuan, N. Zhou, S. Yu, H. Huang, Z. Chen, and F. Xia, “Higher-order structure based anomaly detection on attributed networks,” in *2021 IEEE International Conference on Big Data (Big Data)*. IEEE, 2021, pp. 2691–2700.
- [49] H. Schütze, C. D. Manning, and P. Raghavan, *Introduction to information retrieval*. Cambridge University Press Cambridge, 2008, vol. 39.